Research, Society and Development, v. 10, n. 4, e15110412831, 2021
(CC BY 4.0) | ISSN 2525-3409 | DOI: http://dx.doi.org/10.33448/rsd-v10i4.12831

Development of CuO-based oxygen carriers supported on diatomite and kaolin for chemical looping combustion

Desenvolvimento de transportadores de oxigênio a base de CuO suportado em diatomita e caulim para combustão por recirculação química

Desarrollo de transportadores de oxígeno a base de CuO soportado por diatomita y caolín para combustión por recirculación química

Received: 02/10/2021 | Reviewed: 02/14/2021 | Accept: 03/26/2021 | Published: 04/03/2021

Romário Cezar Pereira da Costa
ORCID: https://orcid.org/0000-0002-1488-8536
Universidade Federal do Rio Grande do Norte, Brazil
E-mail: romariopfg@hotmail.com
Rebecca Araújo Barros do Nascimento
ORCID: https://orcid.org/0000-0002-4185-9802
Universidade Federal do Rio Grande do Norte, Brazil
E-mail: rebeccaabn@hotmail.com
Dulce Maria de Araújo Melo
ORCID: https://orcid.org/0000-0001-9845-2360
Universidade Federal do Rio Grande do Norte, Brazil
E-mail: daraujomelo@gmail.com
Dener Silva Albuquerque
ORCID: https://orcid.org/0000-0003-1892-1783
Universidade Federal do Rio Grande do Norte, Brazil
E-mail: dener_rn@yahoo.com.br
Rodolfo Luiz Bezerra de Araújo Medeiros
ORCID: https://orcid.org/0000-0002-3072-1250
Universidade Federal do Rio Grande do Norte, Brazil
E-mail: rodolfoluiz@gmail.com
Marcus Antônio de Freitas Melo
ORCID: https://orcid.org/0000-0003-3697-2859
Universidade Federal do Rio Grande do Norte, Brazil
E-mail: mafm.ufrn@gmail.com
Juan Adánez
ORCID: https://orcid.org/0000-0002-6287-098X
Instituto de Carboquimica, Espanha
E-mail: jadanez@icb.csic.es

Abstract
Chemical Looping Combustion (CLC) technology has emerged as a promising alternative capable of restricting the effects of global warming due to anthropogenic gas emissions, especially CO_2, through its inherent capture. This study aims to synthesize and evaluate Cu-based oxygen carriers supported on natural materials such as diatomite and kaolin, through the incipient wet impregnation method for CLC process applications. Oxygen carriers were characterized by X-ray diffraction (XRD), temperature-programmed reduction (TPR), and scanning electron microscopy with surface energy dispersive x-ray spectroscopy (SEM-EDS). The mechanical strength of the two oxygen carrier particles was determined after the sintering procedure resulting in high crushing force. Reactivity of oxygen carriers was evaluated in a thermobalance with CH4 and H2 gases. Different reaction pathways were attempted when undergoing the redox cycles: total direct reduction of CuO to Cu^0 for Cu-K and partial reduction of CuO to Cu_2O and CuO to Cu-D. However, the highest reactivity and reaction rate was achieved in Cu-D due to the pore structure of diatomite, the chemical composition and the resulting interaction between CuO and the support. H_2 gas reactivity tests showed a higher conversion rate and greater stability between cycles for both oxygen carriers. Thus, the reducible CuO content present in Cu-Diatomite during the reactivity test with H_2 as the fuel gas was ideal for achieving high solids conversion, tendency for greater stability and a higher reaction rate.
Keywords: CO_2 capture; Chemical looping combustion; Oxygen carriers; Copper; Diatomite; Kaolin.

Resumo
A tecnologia de Combustão com recirculação química (CLC) surgiu como uma alternativa promissora capaz de restringir os efeitos do aquecimento global devido às emissões de gases antropogênicos, principalmente CO_2, por meio de sua captura inerente. Este estudo tem como objetivo sintetizar e avaliar carreadores de oxigênio à base de Cu suportados em materiais naturais como diatomita e caulim, através do método de impregnação úmida incipiente para

aplicações em processos CLC. Os portadores de oxigênio foram caracterizados por difração de raios-X (XRD), redução à temperatura programada (TPR) e microscopia eletrônica de varredura com espectroscopia de energia de superfície dispersiva de raios-X (SEM-EDS). A resistência mecânica dos transportadoras de oxigênio foi determinada após o procedimento de sinterização, resultando em alta força de esmagamento. A reatividade dos carreadores de oxigênio foi avaliada em termobalança com os gases CH_4 e H_2. Diferentes vias de reação foram analisadas durante os ciclos redox: redução direta total de CuO para Cu^0 para Cu-K e redução parcial de CuO para Cu_2O e CuO para Cu-D. No entanto, a maior reatividade e taxa de reação foram alcançadas para o Cu-D devido à estrutura porosa da diatomita, à composição química e à interação resultante entre o CuO e o suporte. Os testes de reatividade com o gás H_2 mostraram uma maior taxa de conversão e maior estabilidade entre os ciclos para ambos os transportadores de oxigênio. Assim, o teor de CuO redutível presente na Cu-D durante o teste de reatividade com H_2 como gás combustível foi ideal para obtenção de alta conversão dos sólidos, tendência a maior estabilidade e maior taxa de reação.
Palavras-chave: Captura de CO_2; Combustão por recirculação química; Transportadores de oxigênio; Cobre; Diatomita; Caulim.

Resumen
La tecnología de combustión con transportadores sólidos de oxígeno (CLC) ha surgido como una alternativa prometedora capaz de restringir los efectos del calentamiento global por emisiones de gases antropogénicos, principalmente CO_2, a través de su captura inherente. Este estudio tiene como objetivo sintetizar y evaluar transportadores de oxígeno basados en Cu apoyados en materiales naturales como la diatomita y el caolín, utilizando el incipiente método de impregnación húmeda para aplicaciones en procesos CLC. Los portadores de oxígeno se caracterizaron por difracción de rayos-X (XRD), reducción com temperatura programada (TPR) y microscopía electrónica de barrido con espectroscopía de energía superficial dispersiva de rayos-X (SEM-EDS). La resistencia mecánica de los portadores de oxígeno se determinó después del procedimiento de sinterización, lo que resultó en una alta fuerza de trituración. La reactividad de los portadores de oxígeno se evaluó en termobalance con los gases CH_4 y H_2. Se analizaron diferentes vías de reacción durante los ciclos redox: reducción total directa de CuO a Cu^0 para Cu-K y reducción parcial de CuO a Cu_2O y CuO para Cu-D. Sin embargo, la mayor reactividad y velocidad de reacción se logró para Cu-D debido a la estructura porosa de la diatomita, la composición química y la interacción resultante entre CuO y el soporte. Las pruebas de reactividad con gas H_2 mostraron una mayor tasa de conversión y una mayor estabilidad entre ciclos para ambos transportadores de oxígeno. Así, el contenido reducible de CuO presente en Cu-D durante la prueba de reactividad con H_2 como gas combustible fue ideal para obtener una alta conversión de sólidos, con tendencia a una mayor estabilidad y mayor velocidad de reacción.
Palabras clave: Captura de CO_2; Combustión con transportadores sólidos de oxígeno; Transportadores de oxigênio; Diatomita; Caolín.

1. Introduction

Sustainability is one of the most important and necessary challenges for societies today. However, the climate change being suffered by the planet should be a warning to this factor. Carbon dioxide (CO_2) is a long-lived anthropogenic gas in the atmosphere and there is an intensification of the effects of global warming due to its progressive emission from fossil fuel combustion processes (Takht & Saeed, 2014; Fernandes *et al*., 2019; Oliveira *et al.*, 2020; Gomes *et al*., 2021). The Paris Agreement was established in order to limit these effects, requiring the decarbonization of the world's energy systems, limiting the average global temperature increase to 2 °C for the next century. In order to achieve this goal, Chemical Looping Combustion (CLC) has emerged as a promising technology for CO_2 capture in power plants and industrial applications with low energy penalty compared to other competing CO_2 capture and storage (CCS) technologies (Adánez-Rubio *et al*., 2018; Adánez *et al*., 2018; McGlashan *et al*., 2012; Wang, Yan *et al*., 2018).

Figure 1. Basic scheme of CLC process.

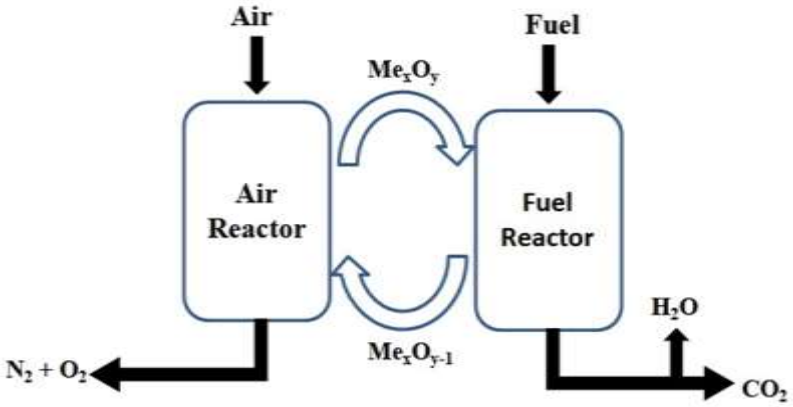

Source: Adapted from Adanez *et al*. (2012).

The Figure 1 show the CLC technology. This system describes cyclic redox processes between two interconnected reactors and is based on the use of a metal oxide (M_xO_y), known as an oxygen carrier (OC), to transfer the required oxygen from the air (Reaction 1) and oxidize the fuel to CO_2 and H_2O (Reaction 2) to avoid direct contact between the air and fuel. Its main advantage is the inherent capture of CO_2, bypassing the energy penalty. Finding oxygen carriers with good physicochemical properties is the critical point for CLC technologies. OCs require high fuel reactivity, excessive oxygen carrying capacity, high friction and agglomeration resistance, low toxicity and low cost (Zhang *et al*., 2019). Based on these characteristics, Adanéz and colleagues (Adanez *et al.*, 2012) reviewed possible Ni, Fe, Cu, Co and Mn oxides and probable inert materials as supports, for example SiO_2, Al_2O_3, TiO_2, ZrO_2, to improve the reactivity and life time of oxygen carriers.

$Me_xO_{y-1} + 1/2O_2 \rightarrow Me_xO_y$ (Reaction 1)

$(2n+m)Me_xO_x + C_nH_{2m} \rightarrow (2n+m)Me_xO_{y-1} + mH_2O + nCO_2$ (Reaction 2)

In addition, there is great flexibility in fuel characteristics, making the use of gaseous, liquid and solid fuels viable. The use of solid fuels such as coal and biomass has been of great interest, as coal will continue to be an important source of energy in the medium term, generating neutral emissions (Takht & Saeed, 2014). Moreover, the use of biomass waste triggers negative emissions due to the intrinsic balance of biomass combined with CO_2 capture and storage techniques (Bioenergy with Carbon Capture and Storage - BECCS) (Adánez *et al*., 2018; Mendiara *et al.*, 2018).

In-Situ Gasification Chemical Looping (iG-CLC) and Chemical Looping with Oxygen Uncoupling (CLOU) are proposed solid fuel CLC processes in which gas-solid reactions occur. In iG-CLC technology, solid fuel is first gasified in situ to synthesis gas ($CO + H_2$) and this reacts with the OC in the fuel reactor (Wang *et al.*, 2018). On the other hand, the CLOU process requires a suitable oxygen carrier capable of reversibly releasing $O_{2(g)}$, having oxygen equilibrium partial pressure at high temperatures (800-1000 °C), for example, CuO, Mn_2O_3 and Co_3O_4 (Abad *et al*., 2012; Adánez-Rubio *et al*., 2017; Gayán *et al*., 2012). In this case, solid fuel is burned by gaseous oxygen which is decoupled from the OC in the fuel reactor. The main advantage of the CLOU process over the iG-CLC is that direct burning of solid fuel promotes faster combustion as it eliminates the slow coal gasification step (Abad *et al.*, 2012; Adánez-Rubio *et al*., 2013; Adánez-Rubio *et al*., 2017).

Cu-based oxygen carriers were reviewed and studied by (Adánez-Rubio *et al.*, 2013; Adánez-Rubio *et al*., 2011; Adanez *et al*., 2012; de Diego *et al*., 2005; Forero *et al*., 2009), and showed high reactivity, high reaction rates, and oxygen carrying capacity, and did not show thermodynamic restrictions for complete conversion of fuel to CO_2 and H_2O. In combining with inert supports such as Al_2O_3, bentonite, MgO, $MgAl_2O_4$, SiO_2, and TiO_2, it is possible to achieve an OC with high mechanical stability and low friction rate. However, problems with agglomeration is a potential issue due to the low melting

temperature of the Cu^0 (1085 °C). Thus, iG-CLC and CLOU can be used with different parameters to prevent this problem. In the CLOU approach, the present redox system is CuO/Cu_2O according to Reaction 3 in order to avoid generating metallic Cu, so that high temperatures are used (900-950 °C) due to the Cu_2O (1235 °C) melting temperature, and therefore the OC has a higher CuO content. In the iG-CLC process, the approached redox system is CuO/Cu according to Reactions 4-5, but the OC has lower CuO content (≤ 21 wt%) and low reaction temperature (≤ 850 °C) due to the melting temperature of Cu (1083 °C) (Wang *et al.*, 2018).

$4CuO \rightarrow O_2 + 2Cu_2O$ (Reaction 3)

$CuO + H_2 \rightarrow H_2O + Cu$ (Reaction 4)

$4CuO + CH_4 \rightarrow 2H_2O + CO_2 + 4Cu$ (Reaction 5)

In addition, the use of Cu-based synthetic oxygen carriers with chemical composition and controllable physical structure is expensive and difficult to produce (Zhang *et al.*, 2019). Thus, a natural support such as diatomite and kaolin which have high mechanical strength, high porosity, high availability in Brazil and low cost, is of interest as supports for CLC applications in fluidized bed reactors due to their highly open porous structure in combination with their high mechanical properties, minimizing the cost of developing large-scale Cu-based oxygen carriers (Liu *et al*., 2019; Van Garderen *et al*., 2012; Van Garderen *et al.*, 2014). It is also important to consider that both materials are mainly composed of Al_2O_3 and SiO_2, and the proportion of these two phases in these materials vary, which opens a discussion about the different types of materials which can be formed when subjected to temperatures above 900 °C (De Freitas *et al.*, 2011; McGlashan *et al.*, 2012; Pio *et al.*, 2018; Pio *et al.*, 2016; Santos *et al.*, 2017).

Song *et al.* (2014) synthesized commercially supported silica and alumina oxygen carriers by the dry impregnation method and significant differences were observed in the CuO conversion rate and cycle stability in operation at 950 °C (Song *et al*., 2014). However, Van Garderen *et al.* (2014) investigated the performance of CuO-based OC supported on a range of substrates with different macropore (SiO_2) and mesopore (γ-Al_2O_3) combinations, and concluded that CuO supported on a combination of mesopores and macropores have better redox performance compared to synthetic supports with a single pore size distribution (Van Garderen *et al*., 2014). In this perspective, the purpose of this work is to evaluate the influence of natural supports (kaolin and diatomite) as sources of silica and alumina on the reactivity of Cu-based oxygen carriers obtained through incipient wet impregnation, aiming toward its use in CLC processes with solid fuels.

2. Methodology

2.1 Preparation of the Oxygen Carriers

The Cu oxygen carriers used in this work were prepared by incipient wet impregnation using $Cu(NO_3)_2.3H_2O$ (VETEC, PA = 99%) and kaolin and diatomite natural materials collected in the state of Rio Grande do Norte, Brazil, in the particle size range 100-300 μ to be used as supports. Gayán et al. (2012) studied the incipient wet impregnation technique, which consists of obtaining a more concentrated nitrate solution of the metal to be impregnated (active phase). For this, a saturated solution of metallic nitrate at 80 ºC is prepared, where the solute is dissolved in its own hydration water, in order to obtain a greater amount of solute per unit volume. The mass of the hydrated salt is weighed in the balance, after dissolving the salt at 80 ºC we obtain the final volume and, thus, the concentration of the copper nitrate solution (Gayán *et al.*, 2012).

Gayán et al. (2012) studied the incipient wet impregnation technique, which consists of obtaining a more concentrated nitrate solution of the metal to be impregnated (active phase). For this, a saturated solution of metallic nitrate at 80 ºC is prepared, where the solute is dissolved in its own hydration water, in order to obtain a greater amount of solute per unit volume.

The mass of the hydrated salt is weighed in the balance, after dissolving the salt at 80 ºC we obtain the final volume and, thus, the concentration of the copper nitrate solution (Gayán et al., 2012).

Wang *et al*. (2017) found that the formation of Cu^0 provides an agglomeration of Cu-based OCs in the CLC process. However, this problem can be avoided by using a low CuO content (Wang *et al.*, 2017). Thus, the mass fraction used was below 20%wt CuO. The impregnation procedure consisted of mechanically mixing a 5 M copper nitrate solution with the porous supports at 80 °C. Three impregnations were performed on each material to achieve the desired mass fraction, yielding a final volume of 0.42 mL and 0.30 mL of $Cu(NO_3)_2.3H_2O$ per gram of Kaolin and Diatomite, respectively. There was a heat treatment at 550 °C/1 h after each of the first two impregnations, but the samples were calcined at 1100 °C/1 h at the end of the last impregnation with the objective of achieving high mechanical strength.

Table 1. Properties of Cu-based oxygen carriers.

Suport		**OCs**					
	Oxides (%)		**Oxides (%)**	**CuO reducible (%)**	**Phase (DRX)**	**R_{oc}**	**Mechanical strength (N)**
Kaolin	50.10 % SiO_2 48.91 % Al_2O_3 0.67 % K_2O 0.214 % Fe_2O_3	Cu-K	12.92 % CuO 37.27 % SiO_2 48.81 % Al_2O_3	12.58 %	CuO, SiO_2, Al_2SiO_5	2.53	2.33
Diatomite	67.55 % SiO_2 31.03 % Al_2O_3 0.77 % K_2O 0.429 % Fe_2O_3	Cu-D	22.85 % CuO 57.57 % SiO_2 19.58 % Al_2O_3	18.94 %	CuO, SiO_2, Al_2O_3	3.81	2.96

Source: Authors (2021).

The composition of calcined Cu samples was determined by X-ray Fluorescence. Table 1 shows the XRF analysis results of the supports and OC, including their main properties.

2.2 Characterization of the Oxygen Carriers

Physical and chemical characterization was performed on oxygen carrier particles. The chemical composition of the samples was determined by X-Ray Fluorescence on a Shimadzu Rayny 720 targeting an Rh anode, 50 kV voltage, Si/Li detector. The identification of the crystalline chemical phases was performed by X-ray Diffraction (XRD) using a Shimadzu XRD-7000 X-ray diffractometer with Cukα radiation (λ = 1.5409 Å). The Joint Committee on Power Diffraction Standards was used to designate the crystalline phases. The structure refinement was performed by applying the Rietveld treatment using MAUD software.

The temperature-programmed reduction (TPR) profile of the OCs was evaluated on a Micromeritics AUTOCHEM II 2920 equipped with a TCD (Thermal Conductivity Detector). The analyzes were conducted by varying the temperature from 100 to 900 °C under 50 $mL.min^{-1}$ flow of a 10% H_2 Argon mixture. It was possible to estimate the oxygen carrying capacity of metallic oxides (R_O) through the consumption of H_2 according to the equations below.

$$C_{H_2\,(mol)} = C_{H2\left(\frac{cm^3}{g}\right)} \times 1ml \times \frac{1L}{1000mL} \times \frac{1mol}{22.4L} \quad \text{(Equation 1)}$$

$$R_O = \frac{m_{oxi} - m_{red}}{m_{oxi}} = \frac{\Delta m}{m_{oxi}} \quad \text{(Equation 2)}$$

$$\Delta m = C_{H2\,(mol)} \times \frac{16g}{mol} \quad \text{(Equation 3)}$$

$$R_{OC} = X_{OC} \times R_O \quad \text{(Equation 4)}$$

In which: $C_{H_2\,(mol)}$ represents the consumption of H_2 per mol, $C_{H2}\left(\frac{cm^3}{g}\right)$ is the experimentally consumed volume of H_2, m_{oxi} and m_{red} is the oxygen carrier mass when fully oxidized and reduced, respectively, R_{OC} is the oxygen carrying capacity of materials, X_{OC} is the fraction of the active phases present in the carriers. The mechanical strength of the particles was determined using a Shimpo FGN-5X dynamometer by averaging 20 measurements of the force required to fracture the particle. The microstructure and distribution of the CuO phase within the particles was analyzed by scanning electron microscopy (SEM) on a Zeiss DSM 942 microscope equipped with an Oxford Link-Isis X-ray Dispersive Energy Analyzer (EDX).

2.3 Oxygen Carrier Reactivity Test

Reactivity tests of oxygen carriers were performed on a thermogravimetric analyzer (TGA) (CI Eletronics), with experimental setup shown in Figure 2.

Figure 2. Schematic diagram of the experimental thermobalance configuration.

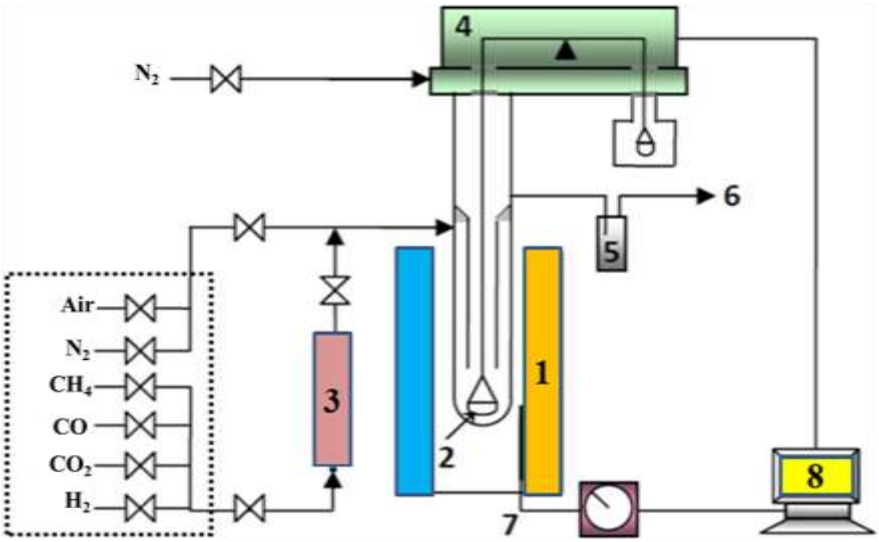

Source: Authors (2021).

In Figura 2: (1) oven; (2) Pt basket with OC; (3) vaporizer; (4) microbalance; (5) condenser; (6) gas outlet; (7) temperature control; and (8) data collector.

In the experiments, 50 mg of the sample was placed in a platinum mesh basket and introduced into a reactor in the form of a quartz tube arranged in an oven operating at a temperature of 950 °C. Upon reaching the operating temperature and system stability, the samples were subjected to the desired reduction and oxidation conditions, alternately and to preserve each step, avoiding reactive gas mixing, and a N_2 flow was introduced for 2 min at the end of each reaction. CH_4 and H_2 were used as reducing gases, synthetic air as oxidizing gas and nitrogen to purge the system, kept at a flow of 25 nL/h throughout the reaction time. The gas composition for the reduction process was 15% of CH_4, 20% H_2O, 65% N_2 or 15% H_2, 85% H_2O, and the gas used for the oxidation process was 100% air. The temperature and weight of the sample were recorded continuously on

a computer. It is also important to have a nitrogen flow of 9 nL/h to the head in this system, keeping it free of reaction gases, preventing corrosion of the thermobalance electronics.

3. Results and Discussion

3.1 Reactivity of the OCs with CH_4 and H_2 in the TGA

Figure 3*a* and *b* show the conversion of oxygen carrier as a function of time over three reactivity test cycles in TGA with hydrogen (15% H_2 + 85% N_2) and methane (15% CH_4 + 20% H_2O +65% N_2) as fuel.

The conversions obtained by Cu-K and Cu-D were calculated from the possible redox reactions involved (reactions 6-11), according to their oxidation degree and in terms of sample weight variation, as shown in Figures 4*a* and *b*.

$$CuO + H_2 \rightarrow H_2O + Cu \quad \text{(Reaction 6)}$$

$$2CuO + H_2 \rightarrow H_2O + Cu_2O \quad \text{(Reaction 7)}$$

$$Cu_2O + H_2 \rightarrow H_2O + 2Cu \quad \text{(Reaction 8)}$$

$$4CuO + CH_4 \rightarrow 2H_2O + CO_2 + 4Cu \quad \text{(Reaction 9)}$$

$$Cu_2O + 1/2O_2 \rightarrow 2CuO \quad \text{(Reaction 10)}$$

$$2Cu + O_2 \rightarrow 2CuO \quad \text{(Reaction 11)}$$

As seen in Figure 4, the largest mass variation for both fuels was obtained with copper oxide supported on diatomite (Cu-D) particles. With CH_4 as fuel, it is observed that there is an increase in mass variation over the cycles for Cu-K. It is also noticeable that the two oxygen carriers showed greater constancy during the three cycles with H_2 as fuel. It is reported that the reduction reactions occurred in two steps in both samples; the first when there is only $N_{2(g)}$ atmosphere, which involves reactions of the CLOU process, causing the transformation of $CuO \rightarrow Cu_2O$, and the second when there is the supply of $H_{2(g)}$ or $CH_{4(g)}$ as combustible gases. These reactions with the reactive gases are equivalent to the reactions of the iG-CLC process, causing the reduction $CuO \rightarrow (Cu_2O) \rightarrow Cu^0$. Note that the mass loss in the first step related to the CLOU process was higher for Cu-D. Therefore, the experiment was performed at 950 °C due to the Cu_2O melting temperature (1235 °C), which is formed during the inert period between oxidation and reduction.

Figure 3. Conversion curves obtained during reactivity test for Cu-K and Cu-D with a) H_2 and b) CH_4 as fuels.

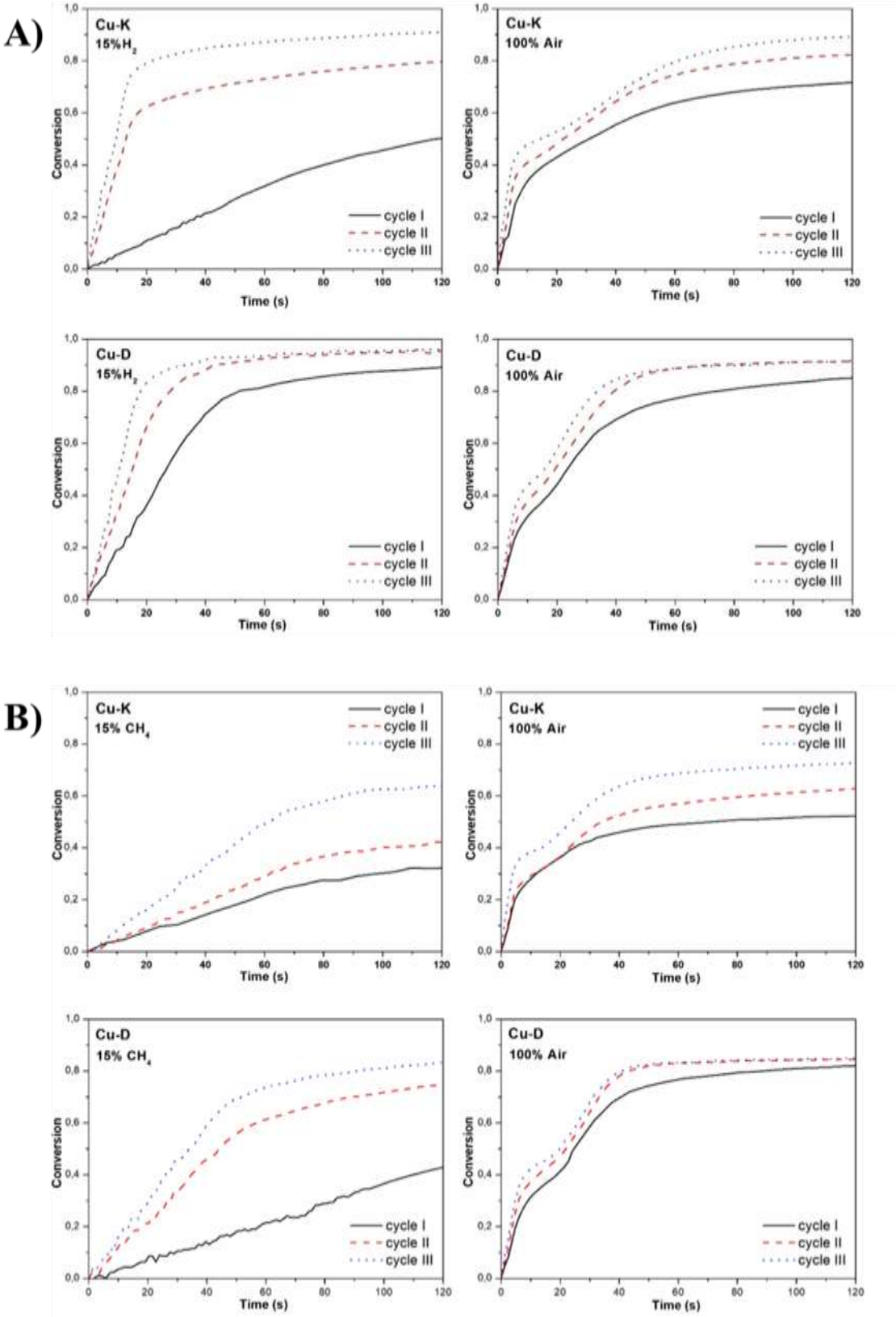

Source: Authors (2021).

Figure 4. Mass variations during reduction and oxidation reactions for Cu-K and Cu-D with a) CH_4 and b) H_2 as fuels.

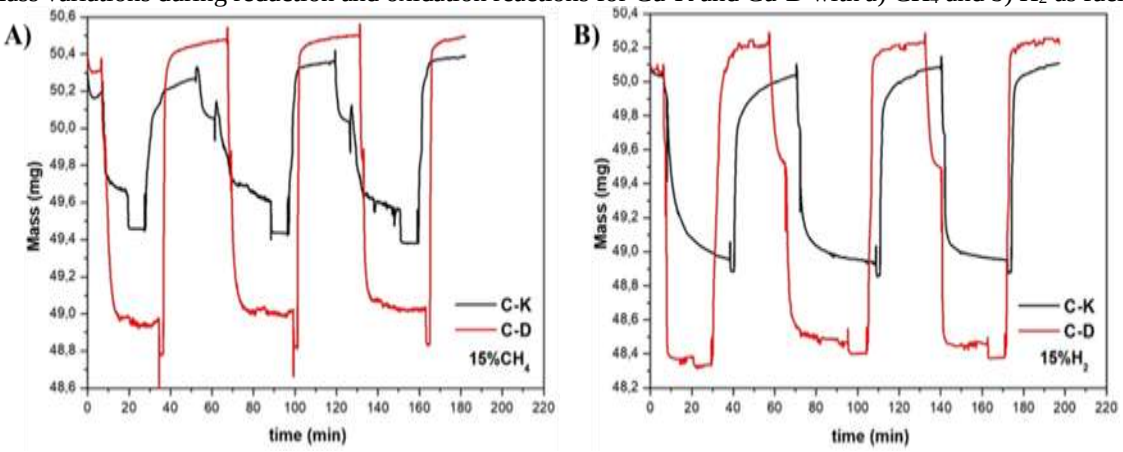

Source: Authors (2021).

The conversion rate calculated for Copper oxide supported on diatomite and kaolin (Figures 3*a* and *b*) shows that there is an increase in reactivity during the three redox cycles, but stability after the third cycle cannot be stated. Early reductions have a slower reaction rate depicting activation of the materials. This is due to the resulting changes in the structure of the fresh oxygen carriers during the first reduction reaction, with the formation of different copper oxides after regeneration in the oxidation step (Wang *et al.*, 2017). The higher reactivity presented by Cu-D with CH_4 and H_2 compared to Cu-K may be due to the porous structure of diatomite, contributing to the reduction of CuO particle agglomeration, leaving them firm on the surface of this support, and consequently increasing the surface area and its oxygen release capacity. In contrast, CuO particles in Cu-K were free to migrate on the surface, and the three successive cycles show greater differences in reactivity in search of stability.

Through the different inclinations, it is also possible to observe that the CuO redox process which occurs in diatomite is faster than in the kaolin support. As the microstructure of these two supports is similar, the resulting effect on reactivity and reaction rate is primarily based on variation in chemical composition and the interaction between CuO and the support (Adánez *et al.*, 2004). But oxygen carriers generally exhibited a higher reaction rate for reduction compared to the reaction rate for oxidation, as noted by Pio *et al.* (2017), probably due to the diffusive effects inside the oxygen carrier particles. Moreover, a higher reaction rate for gaseous fuel is obtained with H_2 than with CH_4 in the same concentration (15%). This can be explained by the reaction stoichiometry, which has a stoichiometry of 1:1 with H_2, while it is 1:4 with CH_4 (Pio *et al.*, 2017).

The evolution of oxygen carrying capacity was evaluated over time for the three cycles, according to Table 2.

Table 2. Oxygen carrying capacity of oxygen carriers during H_2 fuel reactivity test.

		Cycle I	Cycle II	Cycle III
Cu-K	*Reduction*	2,43	2,48	2,53
	Oxidation	2,43	2,58	2,59
Cu-D	*Reduction*	3,51	3,76	3,80
	Oxidation	3,90	3,76	3,81

Source: Authors (2021).

In Table 2 is observed that there are small variations with an increase of R_{oc} at each cycle. These values correspond to the amount of oxygen required to completely convert the fuel into CO_2 and H_2O. Wang *et al.* (2017) investigated the R_{oc} of an oxygen carrier prepared via the impregnation method with a 40%wt. copper oxide supported on natural porous material (olivine - CuO/Olivine), achieving a maximum value of 3.59% in its tenth cycle of the CLC process, concluding that CLC tests

weakly affected oxygen carrying capacity (Wang *et al.*, 2017). This result is higher than Cu-K R_{oc}, but lower than Cu-D in the third cycle, emphasizing that there is a lower percentage of CuO impregnated in these carriers.

3.2 Characterizations of the oxygen carriers

The XRD patterns corresponding to the in natura, kaolin and diatomite supports are shown in Figure 5.

Figure 5. X-ray diffractograms of kaolin and diatomite supports.

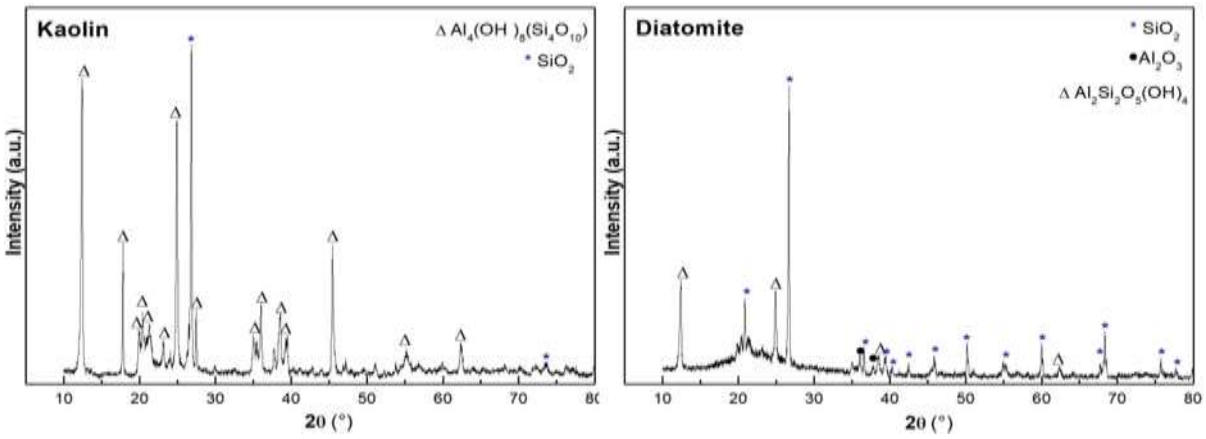

Source: Authors (2021).

According to Figure 5, the kaolin sample showed main crystalline phases for kaolinite ($Al_4(OH)_8(Si_4O_{10})$ - ICSD 063316), with the main peak at 25º, and silica (SiO_2 - ICSD 062404) with the main peak at 26.57°. In the diatomite sample, the silica phase (SiO_2 - ICSD 062404) was also detected with considerably higher intensity than the alumina (Al_2O_3 - ICSD 082504) and aluminosilicate phases ($Al_2Si_2O_5(OH)_4$ – ICSD).

An X-ray Diffraction analysis and fresh oxygen carrier patterns reduced to 10% H_2 gas and oxidized (after the third thermobalance cycle) are shown in Figure 6 to understand the reaction pathways of Cu oxide supported on natural materials (kaolin and diatomite).

The diffractograms of the fresh oxygen carrier particles (Figure 6) revealed the presence of CuO (ICSD 087124) as the main active phase with higher intensity peaks at 35.54° and 38.69°. The inert SiO_2 (ICSD 062404) and Al_2SiO_5 (ICSD 100451) phases were also identified in Cu-K OC. The calcination temperature (1100 °C) to obtain this oxygen carrier caused the kaolinite to dehydrate, converting it to matecaulinite ($Al_2O_3.2SiO_2$) when it reached temperatures above 510°C; while it favored the formation of Al_2SiO_5 aluminosilicate above 900 °C, according to reaction 12. It is observed that the Cu-K sample did not show interaction phases between CuO and SiO_2 present in kaolin, otherwise this interaction could result in a reduction of the oxygen carrying capacity (R_{oc}) of this material (Song et al., 2014). Inert phases were also identified as SiO_2 (ICSD 062404) and Al_2O_3 (ICSD 082504) in the Cu-D OC diffractogram, and the reaction temperature to obtain this oxygen carrier did not cause the formation of copper silicates and aluminates, which could result in a negative effect on their reactivity in CLC processes. These natural inert supports act to increase the mechanical strength, maintaining the porous structure of the particles at high temperatures, and the aluminosilicate can give a high modulus of rupture and chemical stability to the Cu-K oxygen carrier (García-Labiano *et al.*, 2004; Ma *et al.*, 2017).

$$Al_2O_3.2SiO_2 \xrightarrow{>900°C} Al_2SiO_5 + SiO_2 \qquad \text{(Reaction 12)}$$

Figure 6. X-ray diffractogram of fresh Cu-K and Cu-D reduced to 10% H_2 and oxidized after thermobalance testing.

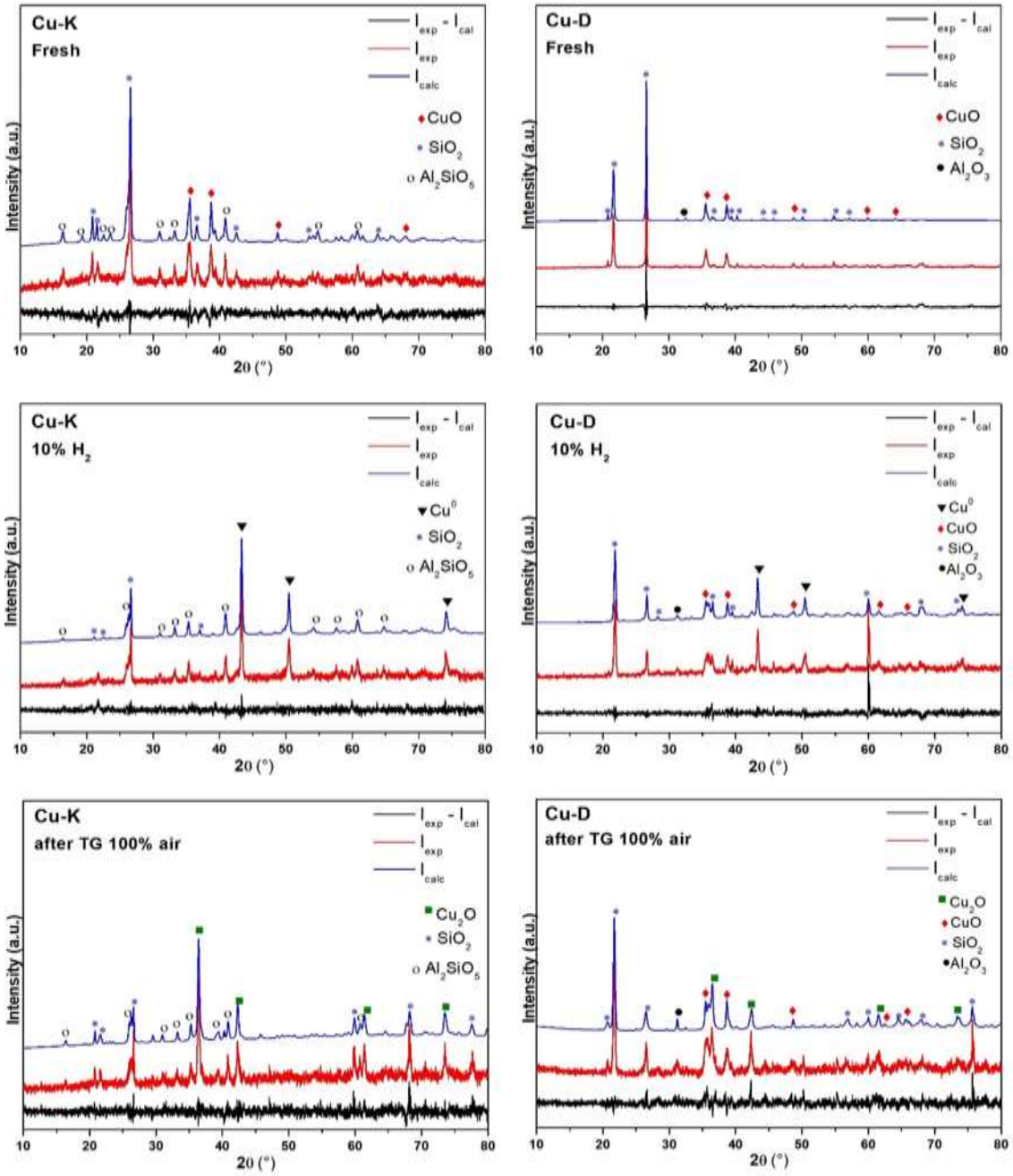

Source: Authors (2021).

The diffractograms of the oxygen carrier particles reduced to 10% H_2 gas indicate that the Cu-K particles underwent uniform reduction reactions and all CuO was reduced to Cu^0 with a peak peak of 43.50°, conforming to reaction 13. In fact, it does not exclude the possibility that Cu_2O exists as an intermediate phase in CuO reduction phase transformations under CLC conditions. However, the diffractogram of the reduced Cu-D particles shows that this reducing condition was not sufficient for the complete reduction of CuO to Cu_2O and/or Cu^0. Table 3 shows the percentage of the crystalline phases of the carriers reduced to 10% H_2 through the Rietveld refinement and proves the conversion of each phase.

$$CuO + H_2 \rightarrow Cu \qquad \text{(Reaction 13)}$$

After the third thermobalance cycle in the reoxidation step, in the diffractograms it is noted that the reduced Cu-K OC particles did not present the fully oxidized copper oxide (CuO) phase. For the Cu-D OC, a mixture of Cu_2O and CuO with 4.90%wt. and 11.66%wt. was identified respectively, according to the data from the Rietveld refinement presented in Table 3. However, the reactivity tests show increased reactivity with increasing number of cycles, so Cu_2O reoxidation does not negatively affect its conversion. This fact may be related to the high reduction rate providing a good final Cu_2O phase conversion (Pio *et al.*, 2018).

Table 3 - Percentage of phases in OCs calcined at 1100 °C (1h) obtained by the Rietveld refinement.

OC	Phases (% wt.)						Crystallinity (%)	Refinament parameters	
	CuO	Cu^0	Cu_2O	Al_2O_3	SiO_2	Al_2SiO_5		Sig	Rwp (%)
Cu-K (Fresh)	12.29	-	-	-	34.66	53.05	54.77	1.28	11.92
Cu-K (10% H_2)	-	23.59	-	-	22.17	54.24	59.77	1.13	13.39
Cu-K (After TG)	-	-	24.89	-	18.00	57.11	73.22	1.21	14.51
Cu-D (Fresh)	20.34	-	-	2.00	77.66	-	79.01	1.71	14.05
Cu-D (10%H_2)	9.91	12.02	-	12.41	65.66	-	77.51	1.28	14.41
Cu-D (After TG)	11.66	-	4.90	6.87	76.57	-	81.39	1.26	12.80

Source: Authors (2021).

In addition, according to the concentration of the crystalline phase obtained by the refinement (as shown in Table 3), different percentages of reducible Cu under CLC conditions present in the samples can refer to an activation step of the materials in the first cycle, so that only the three cycles cannot indicate reliable stability.

Table 4 shows the mechanical strength of the Cu-D and Cu-K particles after being calcined at 1100 °C. According to Adanez *et al.* (2004), the resistance in Newton (N) of the particles depends on the type of metal oxide used as the active phase, its concentration, the support used and the sintering temperature (Adánez *et al.*, 2004). High sintering temperatures generally increase the strength of oxygen carriers. However, this temperature should be limited for copper as it may cause it to melt.

Table 4. Mechanical strength and standard deviation of oxygen carriers at 1100 °C.

OCs	Mechanical strength (N)	Standard deviation
Cu-D	2,96	0,93
Cu-K	2,33	0,81

Source: Authors (2021).

The Table 4 reports that copper oxide exhibits appreciable mechanical strength when using SiO_2 as a support. According to Johansson *et al.* (2004), oxygen carriers with mechanical strength less than 1.0N are unsuitable for use in CLC processes (Johansson *et al.*, 2004).

Thus, it is possible to evidence that the optimization of the mechanical strength of Cu-D and Cu-K particles is the result of the presence of aluminosilicates acting as a support and control for the percentage of active phase impregnated (less than 21%wt. of CuO), favoring the calcination of the OCs at 1100 °C. Cu-D has higher mechanical strength because it has a higher CuO concentration compared to Cu-k. Therefore, both Cu-based oxygen carriers have excellent mechanical strength to be applied in chemical recirculation processes.

Figure 7. Temperature-Programmed Reduction of the Oxygen Carriers: Cu-K and Cu-D.

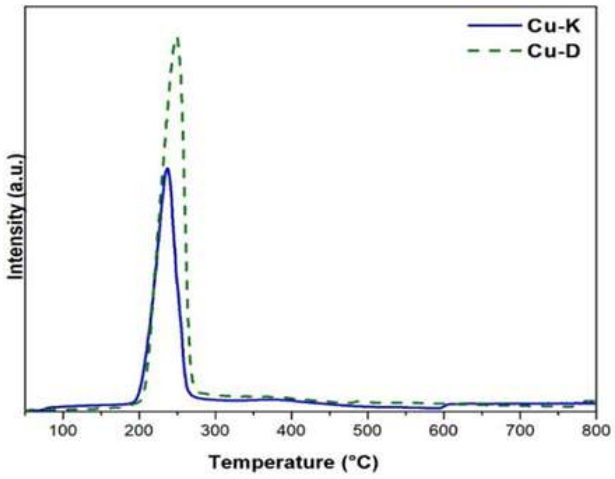

Source: Authors (2021).

Figure 7 shows the H_2-TPR profiles of Cu oxygen carriers. It is observed that there is a single apparent peak in the temperature range of 190-380 °C during the reduction of Cu-K and Cu-D particles. This peak can be attributed to the reduction of a single Cu species ($Cu^{2+} \rightarrow Cu^0$), in accordance with the symmetrical characteristic of the peaks, with a maximum consumption around 240 °C. H_2 consumption was more intense in Cu-D (43.84 cm^3/g) compared to the reduction of Cu-K particles (27.77 cm^3/g) due to the higher percentage of copper oxide present (20.34%), and its wider peak may be associated with a more difficult reduction.

The surface and particle morphology of Cu-K and Cu-D oxygen carriers were assessed by Scanning Electron Microscopy (SEM), as shown in Figure 8 and Figure 9, respectively.

Figure 8. X-ray Dispersive Energy Scanning Electron Microscopy (SEM/EDS) of the surface of the: a) Cu-K and b) Cu-D.

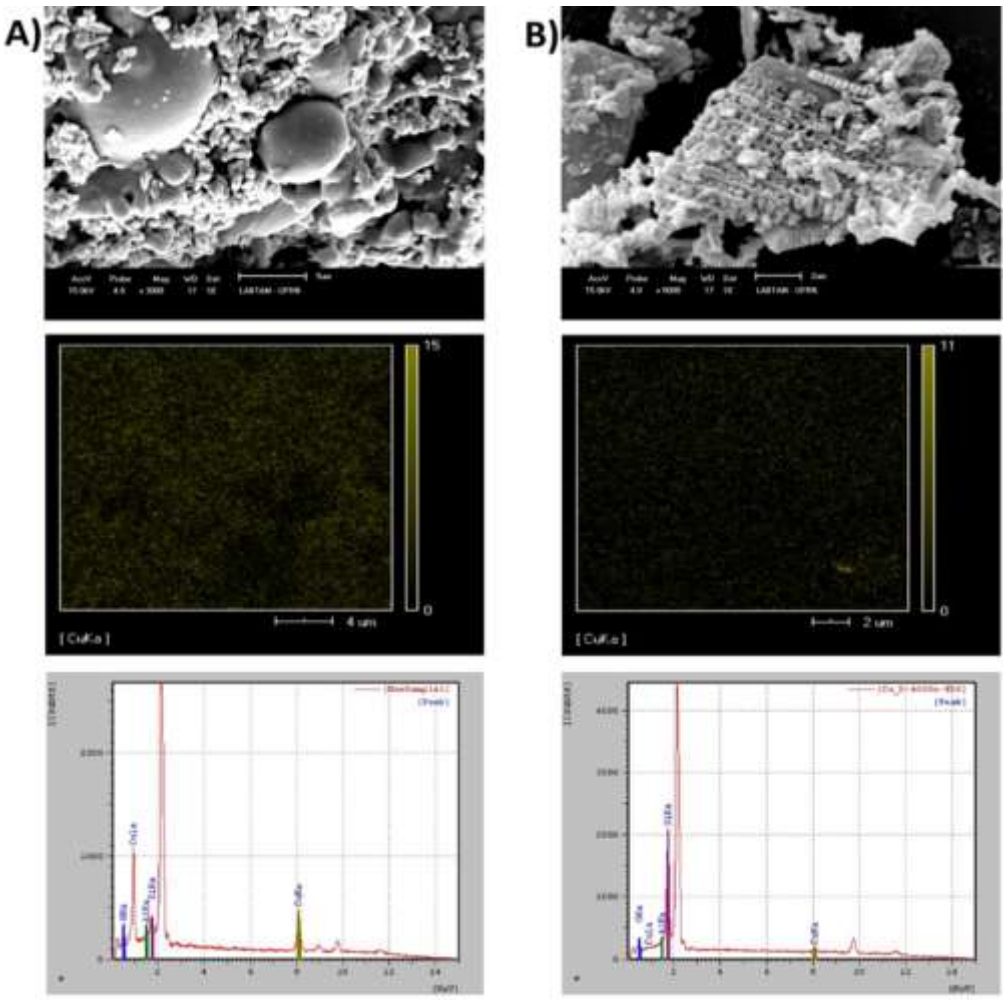

Source: Authors (2021).

As shown in Figures 8*a* and *b*, the Cu-K surface (Figure 8*a*) has a smooth surface with different sized grains and irregularly shaped CuO particles deposited, and the Cu-D surface (Figure 8*b*) is morphologically shaped in the form plates showing well-defined pores with the CuO particles blocking and coating the porous structure. These characteristics are derived from the morphology of the natural kaolin and diatomite supports (Johansson *et al.*, 2004; Maia *et al.*, 2019; Mebreka *et al.*, 2019). It is possible to verify that there is uniform distribution of irregularly shaped CuO particles through the chemical mapping of both surfaces. The uniformity of distribution plays an important role as it favors an increase in surface area, making copper oxide more available on the surface. The presence of Si, Al, Cu and O elements was identified, being consistent with the of XRF and XRD results.

Figure 9. Particle Scanning Electron Microscopy of: a) Cu-K and b) Cu-D.

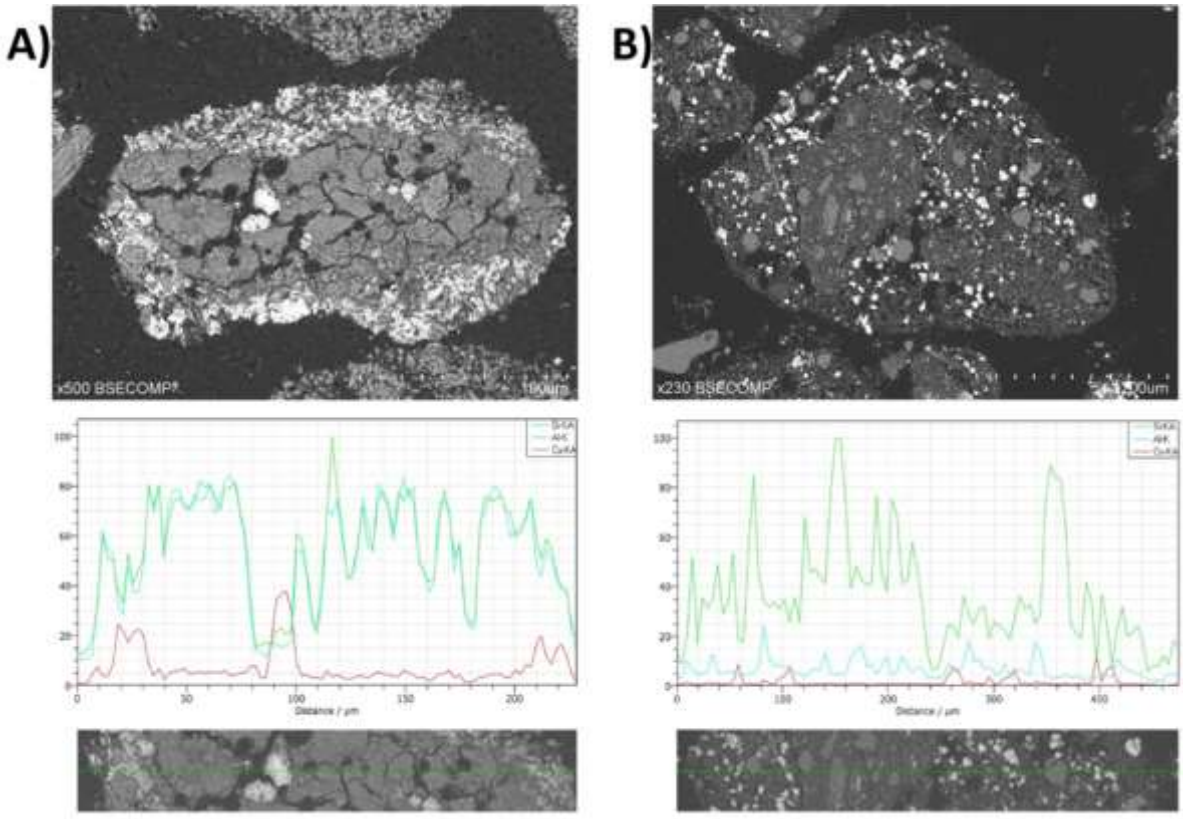

Source: Authors (2021).

Figures 9*a* and *b* show that there are groups of CuO particles within the Cu-K and Cu-D oxygen carrier particles respectively, not showing a uniform distribution of the active phase. However, a study by Wang *et al.* (2017) reveals that the accumulation of CuO particles gradually disappears with an increasing number of redox cycles (Wang *et al.*, 2017). This fact contributes to the increased reactivity of oxygen carriers over the course of reaction cycles.

It was also observed (in Figure 9) that there is a lower CuO content on the Cu-D particle surface compared to the Cu-K particle surface, which induces that copper oxide has penetrated the porous structure of the support. Therefore, although Cu-D has a higher CuO content, a less amount which is present in Cu-K is available to participate in CLC reactions. However, it is important to highlight that the Cu-D reactivity test with CH_4 and H_2 in TGA showed that the percentage of active phase present was ideal to maintain its reactivity during the cycles presented.

4. Conclusion

Reactivities during the reduction and oxidation reactions of Cu-based oxygen carriers (CuO) supported on natural diatomite and kaolin materials were analyzed by thermogravimetry (TGA) and their physicochemical properties by XRD, SEM-EDS, and TPR. The impregnation of CuO particles in the diatomite and kaolin supports did not result in forming copper silicates and aluminates. Moreover, they showed appropriate mechanical strength and uniform distribution of the CuO particles on the surface of the oxygen carriers. Both showed increased reactivity and oxygen carrying capacity when submitted to three redox cycles, but their stability was not reached after the third cycle. This reveals that there are changes in the structure of the oxygen carriers during this reaction period. The regeneration of Cu-K after the third cycle with CH_4 did not lead to the formation of fully oxidized copper oxide and a mixture of Cu_2O and CuO was identified in Cu-D, but failure to obtain fully oxidized CuO did not affect its reactivity during the cycles. Reactivity tests with H_2 gas as the fuel showed a higher conversion

rate and greater constancy between cycles for both oxygen carriers. It was observed that Cu-D presented a higher reactivity and reaction rate in the reduction and oxidation steps, which can be attributed to the pore structure of diatomite, the chemical composition and the resulting interaction between CuO and the support. The percentage of reducible CuO present in Cu-D during the reactivity test with H_2 as fuel gas was ideal for achieving high solids conversion, a greater tendency to stability and a higher reaction rate.

For future work, we can develop a new synthesis route, by which it will improve the mechanical resistance of the oxygen carriers studied in this work. With the improvement of the mechanical resistance of these materials we will have greater stability of the samples during the accomplishment of the multiple redox cycles.

Acknowledgments

The authors wish to thank the Brazilian Federal agencies CAPES (National Council for the improvement of Higher Education Personnel) and CNPq (National Conncil for Scientific and Technological Development) for financial support, and the Instituto de Carboquímica (ICB-CSIC-Spain) for reactivity tests and characterizations.

References

Abad, A., Cuadrat, A., Mendiara, T., García-Labiano, F., Gayán, P., De Diego, L. F., & Adánez, J. (2012). Low-cost Fe-based oxygen carrier materials for the iG-CLC process with coal. 2. *Industrial and Engineering Chemistry Research*, *51*(50), 16230–16241. https://doi.org/10.1021/ie302158q.

Adánez-Rubio, I., Arjmand, M., Leion, H., Gayán, P., Abad, A., Mattisson, T., & Lyngfelt, A. (2013). Investigation of combined supports for cu-based oxygen carriers for chemical-looping with oxygen uncoupling (CLOU). *Energy and Fuels*, *27*(7), 3918–3927. https://doi.org/10.1021/ef401161s.

Adánez-Rubio, I., Gayán, P., García-Labiano, F., de Diego, L. F., Adánez, J., & Abad, A. (2011). Development of CuO-based oxygen-carrier materials suitable for Chemical-Looping with Oxygen Uncoupling (CLOU) process. *Energy Procedia*, *4*, 417–424. https://doi.org/10.1016/J.EGYPRO.2011.01.070.

Adánez-Rubio, I., Izquierdo, M. T., Abad, A., Gayán, P., de Diego, L. F., & Adánez, J. (2017). Spray granulated Cu-Mn oxygen carrier for chemical looping with oxygen uncoupling (CLOU) process. *International Journal of Greenhouse Gas Control*, *65*, 76–85. https://doi.org/10.1016/J.IJGGC.2017.08.021.

Adánez-Rubio, I., Pérez-Astray, A., Mendiara, T., Izquierdo, M. T., Abad, A., Gayán, P., … Adánez, J. (2018). Chemical looping combustion of biomass: CLOU experiments with a Cu-Mn mixed oxide. *Fuel Processing Technology*, *172*(January), 179–186. https://doi.org/10.1016/j.fuproc.2017.12.010.

Adanez, J., Abad, A., Garcia-Labiano, F., Gayan, P., & De Diego, L. F. (2012). Progress in chemical-looping combustion and reforming technologies. *Progress in Energy and Combustion Science*, *38*(2), 215–282. https://doi.org/10.1016/j.pecs.2011.09.001.

Adánez, J., Abad, A., Mendiara, T., Gayán, P., de Diego, L. F., & García-Labiano, F. (2018). Chemical looping combustion of solid fuels. *Progress in Energy and Combustion Science*, Vol. 65, pp. 6–66. https://doi.org/10.1016/j.pecs.2017.07.005.

Adánez, J., De Diego, L. F., García-Labiano, F., Gayán, P., Abad, A., & Palacios, J. M. (2004). Selection of oxygen carriers for chemical-looping combustion. *Energy and Fuels*, *18*(2), 371–377. https://doi.org/10.1021/ef0301452.

de Diego, L. F., Gayán, P., García-Labiano, F., Celaya, J., Abad, A., & Adánez, J. (2005). Impregnated CuO/Al2O3 oxygen carriers for chemical-looping combustion: Avoiding fluidized bed agglomeration. *Energy and Fuels*, *19*(5), 1850–1856. https://doi.org/10.1021/ef050052f.

De Freitas, V. A. A., Lima, J. S. V., & Da Couceiro, P. R. C. (2011). Caracterização e análise estrutural da hidroxisodalita sintetizada a partir de amostras de solo Amazônico. *Ceramica*, *57*(343), 281–287.

Fernandes, T., Hacon, S. S., Novais, J. W. Z., Siguarezi, S. B., Silva, C. J., Alcântara, L. C. S., Curvo, A. D., Fernandes, T. (2019). Poluição do ar e efeitos na saúde de crianças na Amazônia paraense: uma análise bibliométrica. *Pesquisa, Sociedade e Desenvolvimento, 8 (4)*, e4984907. http://dx.doi.org/10.33448/rsd-v8i4.907.

Forero, C. R., Gayán, P., de Diego, L. F., Abad, A., García-Labiano, F., & Adánez, J. (2009). Syngas combustion in a 500 Wth Chemical-Looping Combustion system using an impregnated Cu-based oxygen carrier. *Fuel Processing Technology*, *90*(12), 1471–1479. https://doi.org/10.1016/j.fuproc.2009.07.001.

García-Labiano, F., de Diego, L. F., Adánez, J., Abad, A., & Gayán, P. (2004). Reduction and Oxidation Kinetics of a Copper-Based Oxygen Carrier Prepared by Impregnation for Chemical-Looping Combustion. *Industrial & Engineering Chemistry Research*. https://doi.org/10.1021/ie0493311.

Gayán, P., Adánez-Rubio, I., Abad, A., De Diego, L. F., García-Labiano, F., & Adánez, J. (2012). Development of Cu-based oxygen carriers for Chemical-Looping with Oxygen Uncoupling (CLOU) process. *Fuel*, *96*, 226–238. https://doi.org/10.1016/j.fuel.2012.01.021.

Gomes, D. S., Barbosa, A. S., Santos, T. M., Santos, S. K., Sales Silva, J. H. C., Aquino, I. S. (2021). Cinética de liberação de CO2 e decomposição da fitomassa em sistemas de uso e manejo do solo. *Pesquisa, Sociedade e Desenvolvimento, 10* (1). e9810111413. http://dx.doi.org/10.33448/rsd-v10i1.11413.

Johansson, M., Mattisson, T., & Lyngfelt, A. (2004). *Investigation of FeO with MgAlO for Chemical-Looping Combustion Investigation of Fe2O3 with MgAl 2 O 4 for Chemical-Looping Combustion*. *43*(22), 6978–6987. https://doi.org/10.1021/ie049813c.

Liu, J., Zheng, C., Yue, J., & Xu, G. (2019). Synthesis, characterization and catalytic methanation performance of modified kaolin-supported Ni-based catalysts. *Chinese Journal of Chemical Engineering*. https://doi.org/10.1016/J.CJCHE.2019.04.009.

Ma, J., Tian, X., Zhao, H., Bhattacharya, S., Rajendran, S., & Zheng, C. (2017). Investigation of Two Hematites as Oxygen Carrier and Two Low-Rank Coals as Fuel in Chemical Looping Combustion. *Energy and Fuels*, *31*(2), 1896–1903. https://doi.org/10.1021/acs.energyfuels.6b02101.

Maia, A. Á. B., Dias, R. N., Angélica, R. S., & Neves, R. F. (2019). Influence of an aging step on the synthesis of zeolite NaA from Brazilian Amazon kaolin waste. *Journal of Materials Research and Technology*, *8*(3), 2924–2929. https://doi.org/10.1016/j.jmrt.2019.02.021.

McGlashan, N., Shah, N., Caldecott, B., & Workman, M. (2012). High-level techno-economic assessment of negative emissions technologies. *Process Safety and Environmental Protection*. https://doi.org/10.1016/j.psep.2012.10.004.

Mebreka, A., & , Hadda Rezzaga, Sihem Benayachea, Afef Azzia, Yasmina Taïbib, Sabrina Ladjamaa, Naima Touatia, Azzedine Grida, S. B. (2019). *Effect of chamotte on the structural and microstructural characteristics of mullite elaborated via reaction sintering of Algerian kaolin*.

Mendiara, T., Pérez-Astray, A., Izquierdo, M. T., Abad, A., de Diego, L. F., García-Labiano, F., & Adánez, J. (2018). Chemical Looping Combustion of different types of biomass in a 0.5 kWth unit. *Fuel*, *211*, 868–875. https://doi.org/10.1016/j.fuel.2017.09.113.

Oliveira, M M., Esteves, P. M. S. V., Baía, S. R. D., Dantas, N. S., Silva, V. F. (2020). Análise da produção científica internacional sobre mudanças climáticas e poluição do ar. *Pesquisa, Sociedade e Desenvolvimento*,*9* (10), e1609108314. http://dx.doi.org/10.33448/rsd-v9i10.8314.

San Pio, M. A., Gallucci, F., Roghair, I., & van Sint Annaland, M. (2017). On the mechanism controlling the redox kinetics of Cu-based oxygen carriers. *Chemical Engineering Research and Design*, *124*, 193–201. https://doi.org/10.1016/j.cherd.2017.06.019.

San Pio, M. A., Martini, M., Gallucci, F., Roghair, I., & van Sint Annaland, M. (2018). Kinetics of CuO/SiO2 and CuO/Al2O3 oxygen carriers for chemical looping combustion. *Chemical Engineering Science*, *175*, 56–71. https://doi.org/10.1016/j.ces.2017.09.044.

San Pio, M. A., Roghair, I., Gallucci, F., & van Sint Annaland, M. (2016). Investigation on the decrease in the reduction rate of oxygen carriers for chemical looping combustion. *Powder Technology*, *301*, 429–439. https://doi.org/10.1016/J.POWTEC.2016.06.031.

Santos, K. C. V, Gonçalves, W. P., Silva, V. J., Santana, L. N. L., & Lira, H. L. (2017). Formação de Mulita a Partir de Composições de Caulim e Alumina com Diferentes Tamanhos de Partículas. *Revista Eletrônica de Materiais e Processos*, *3*(2016), 136–142.

Song, H., Shah, K., Doroodchi, E., Wall, T., & Moghtaderi, B. (2014). Reactivity of Al2O3- or SiO2-Supported Cu-, Mn-, and Co-based oxygen carriers for chemical looping air separation. *Energy and Fuels*, *28*(2), 1284–1294. https://doi.org/10.1021/ef402268t.

Takht, M., & Saeed, R. (2014). *Carbon dioxide capture and utilization in petrochemical industry : potentials and challenges*. (27), 63–77. https://doi.org/10.1007/s13203-014-0050-5.

Van Garderen, Noémie, Clemens, F. J., Kaufmann, J., Urbanek, M., Binkowski, M., Graule, T., & Aneziris, C. G. (2012). Pore analyses of highly porous diatomite and clay based materials for fluidized bed reactors. *Microporous and Mesoporous Materials*, *151*, 255–263. https://doi.org/10.1016/J.MICROMESO.2011.10.028.

Van Garderen, Noemie, Otal, E. H., Aneziris, C. G., Graule, T., & Clemens, F. J. (2014). Influence of porous substrate on copper based oxygen carrier efficiency for chemical-looping combustion. *Microporous and Mesoporous Materials*, *190*, 362–370. https://doi.org/10.1016/j.micromeso.2014.02.017.

Wang, K., Yan, X., & Komarneni, S. (2018). CO 2 Adsorption by Several Types of Pillared Montmorillonite Clays. *Applied Petrochemical Research*, *8*(3), 173–177. https://doi.org/10.1007/s13203-018-0206-9.

Wang, P., Means, N., Howard, B. H., Shekhawat, D., & Berry, D. (2018). The reactivity of CuO oxygen carrier and coal in Chemical-Looping with Oxygen Uncoupled (CLOU) and In-situ Gasification Chemical-Looping Combustion (iG-CLC). *Fuel*, *217*(January), 642–649. https://doi.org/10.1016/j.fuel.2017.12.102.

Wang, X., Xu, T., Jin, X., Hu, Z., Liu, S., Xiao, B., & Hu, M. (2017). CuO supported on olivine as an oxygen carrier in chemical looping processes with pine sawdust used as fuel. *Chemical Engineering Journal*. https://doi.org/10.1016/j.cej.2017.07.175.

Zhang, L., Li, K., Gu, Z., Zhu, X., Wei, Y., Li, L., & Wang, H. (2019). Iron-rich copper ore as a promising oxygen carrier for chemical looping combustion of methane. *Journal of the Taiwan Institute of Chemical Engineers*, *101*, 204–213. https://doi.org/10.1016/j.jtice.2019.04.053.